ORIGINAL PAPER

Difference map and its electronic circuit realization

M. García-Martínez · I. Campos-Cantón ·
E. Campos-Cantón · S. Čelikovský

Abstract In this paper we study the dynamical behavior of the one-dimensional discrete-time system, the so-called iterated map. Namely, a bimodal quadratic map is introduced which is obtained as an amplification of the difference between well-known logistic and tent maps. Thus, it is denoted as the so-called difference map. The difference map exhibits a variety of behaviors according to the selection of the bifurcation parameter. The corresponding bifurcations are studied by numerical simulations and experimentally. The stability of the difference map is studied by means of Lyapunov exponent and is proved to be chaotic according to Devaney's definition of chaos. Later on, a design of the electronic implementation of the difference map is presented. The difference map electronic circuit is built using operational amplifiers, resistors and an analog multiplier. It turns out that this electronic circuit presents fixed points, periodicity, chaos and intermittency that match with high accuracy to the corresponding values predicted theoretically.

Keywords Chaotic behavior · Lyapunov exponent · Bifurcation parameter · Bifurcation diagram · Stability analysis

M. García-Martínez (✉) · E. Campos-Cantón
Division de Matemáticas Aplicadas, Instituto Potosino de
Investigación Científica y Tecnológica, Camino a la Presa
San José 2055, 78216 México, México
e-mail: moises.garcia@ipicyt.edu.mx

I. Campos-Cantón
Facultad de Ciencias, Universidad Autónoma de San Luis
Potosí, Zona universitaria, Avenida Salvador Nava S/N,
78290 México, México
e-mail: icampos@fciencias.uaslp.mx

E. Campos-Cantón
Departamento de Físico Matemáticas, Universidad
Autónoma de San Luis Potosí, Zona universitaria, Avenida
Niño Artillero S/N, 78290 México, México
e-mail: eric.campos@ipicyt.edu.mx

S. Čelikovský
Department of Control Theory, Institute of Information
Theory and Automation, Academy of Sciences of the
Czech Republic, Pod vodárenskou věží 4, 18208 Prague,
Czech Republic
e-mail: celikovs@utia.cas.cz

1 Introduction

Iterated maps are simple looking discrete-time dynamical systems which can exhibit transitions from order to chaos. Famous and broadly studied examples of unimodal maps are the tent map and the logistic map, being the subject of constant investigation in many areas such as communication systems [1], generation of pseudo-random sequences [2–4], neural networks [5], switching systems [6] and cryptography [7–11] and part of the interest for these systems is linked to the fact that they provide an easy and academic way to understand how complex and chaotic behavior can arise from simple dynamical models. Even more remarkable is the fact that studies of low-dimensional maps

have proven to be profitable in understanding the basic mechanisms responsible for the appearance of chaos in a large class of dynamical systems.

Furthermore complex behavior may be provided by the so-called bimodal, or even *k*-modal maps, [12]. This paper introduces yet another bimodal map, based on the difference between logistic and tent maps multiplied by a new bifurcation parameter. This new system is therefore called the *difference* one and is carefully analyzed theoretically, numerically and experimentally through electronic circuit.

One of the most useful and widely accepted definition of chaos is the given by Devaney [13], which we will call Devaney-chaos. Roughly speaking, three conditions are required, (1) the sensitive dependence upon the initial condition, (2) the topological transitivity, and (3) the dense distribution of the periodic orbits. The third condition is often omitted for being too stringent [14]. Fortunately, there are other ways to characterize the dynamic behavior, like the result of Li–Yorke [15] which can be used to prove the existence of chaos in a map, the authors state that if there exists a point of period three then there exist points with other periods and the system is chaotic. On the other hand we have the Lyapunov exponents [16–18]. With the aid of their diagnostic, one can measure the average exponential rates of divergence or convergence of nearby orbits in the phase space. In general, sings of the Lyapunov exponents give a qualitative idea of the variety of dynamics that may exhibit, ranging from fixed points via limit cycles and tori to more complex chaotic attractors. Also, bifurcation diagrams are excellent tools to study dynamical behavior and understand mechanisms such as the so-called a cascade of period-doubling bifurcations, encountered qualitatively in many physical systems of interest or mathematical models that have been electronically implemented [19, 20].

Electronic implementation of chaotic systems have been applied to several engineering developments, furthermore they have been of great help to validate certain theories concerning chaos. Since its inception three decades ago, there are different implementations of Chua's circuit [21–23]. Historically seen, Chua's circuit was the first successful physical implementation of a system designed to exhibit chaos [24]. This circuit is the first system rigorously proved to be chaotic [25]. Chua's circuit is a continuous-time dynamical system where chaos can be observed ex-

perimentally. The original Chua's system has a double scroll but the diode has been modified in order to generate chaotic multi-scroll [26]. The behavior of the difference map is simpler than Chua's circuit to comprehend and it has been proved chaotic. The behavior of Chua's oscillator is due to the fact that it contains five different parameters, whereas for difference map is only one. There have been reported several electronic implementations of continuous-time dynamical systems, such systems are based on third-order differential equations see [27–31], but few in the area of discrete-time dynamical systems. Furthermore, discrete-time dynamical systems present advantage and be useful in applications like encryption systems, radar systems, secure communication systems, among others.

Some discrete dynamical systems have been implemented by using digital integrated circuits, for example in [32] presents a digital implementation of the tent map. The problem that arises using digital implementation is that the system only takes a finite number of states. Electronic circuits have been designed, implemented and tested to accurately realize the logistic difference equation [19] or the tent-map difference equation [20] by using analog devices in order to have an infinite number of values that can be visited.

In this paper, we enlarge the set of maps known to be chaotic by presenting a chaotic map based on the difference between the logistic map and the tent map. The difference map, more precisely, enables us to construct a bimodal map which is chaotic in the sense that it has positive Lyapunov exponent. We also present an electronic implementation of the difference map based on analog devices, which at the same time is a good engineering model of the corresponding mathematical system. Through the variation of only one control parameter, one can examine the bifurcation diagram of the realized system and we have been able to reproduce the theoretical diagram with high accuracy.

The possible application of this circuit implementation would be independent analog chaos generator usable for encryption purposes, e.g. as independent device to cipher. In recent years, a growing number of cryptosystems based on continuous systems utilize the idea of synchronization of chaos. However, recent studies show that the performance of continuous systems is very poor and insecure. The insecurity results mainly from the insensitivity of synchronization to systems parameters [33–36] i.e., the synchronization

of a pair of chaotic systems is possible even if they have mismatch parameters.

This paper is organized as follows. In the next section we recall some basic definitions; while Sect. 3 introduces the difference map, including its theoretical and numerical study and presents its properties. Section 4 contains a description of an electronic circuit implementation of the difference map and the experimental bifurcation diagram which matches the theoretically predicted results. Some conclusions and outlook are given in the final section.

2 Basic definitions

This paper aims to contribute in the area of the one-dimensional discrete-time systems, namely to the systems of the form

$$x_{k+1} = f(x_k), \quad k = 0, 1, 2, \ldots, N.$$

Here $x_k \in \Re$ and x_0 is the initial condition, such dynamical system is usually called a *map*, as it is fully determined by its right hand side. To ensure boundedness of trajectories, the study is usually restricted to maps that are mapping some closed interval into itself and without any loss of generality one may consider the closed interval $[0, 1]$ only. The simplest maps are the so-called unimodal maps, while their generalization, the so-called k-modal maps may present even more rich dynamical behaviors, [12].

To be more specific, denote $\mathcal{I} := [0, 1]$ and recall that the *critical point* c of the continuous piecewise smooth map $f(x) : \mathcal{I} \mapsto \mathcal{I}$ is $c \in \mathcal{I}$ where f is differentiable and $f'(c) = 0$.

Remark 1 The critical point c occurs for $f'(c) = 0$ or $f'(c)$ does not exist. But continuous smooth maps always present $f'(c) = 0$.

First, let us repeat the definition of the k-modal map, introduced in [12].

Definition 1 The map $f : \mathcal{I} \mapsto \mathcal{I}$ is called the k-modal one, if it is continuous on $\mathcal{I}$ and it has k critical points denoted by $c_0, c_1, \ldots, c_{k-1}$ in I. Moreover, there exist intervals $\mathcal{I}_i, i = 0, \ldots, k-1, \bigcup_{i=1}^{k} \mathcal{I}_{i-1} = \mathcal{I}$, such that $\forall i = 0, \ldots, k-1$ it holds $c_i \in \mathcal{I}_i$ and $f(c_i) > f(x, \beta), \forall x \in \mathcal{I}_i$ and $x \neq c_i$, where β is a parameter. The case $k = 1$ will be further simply referred

as to the so-called *unimodal* map, while the case $k = 2$ as the *bimodal* one.

Remark 2 The above definition does not constrain a function to have only k critical points. However we only considered those that are local maxima on a subinterval.

Definition 2 The logistic map is defined as

$$f_L(x, \alpha) = \alpha x(1 - x), \tag{1}$$

where parameter $\alpha \in [0, 4] \subset \Re$.

The logistic map was first presented by Verhulst [37] as a model for the growth of species and it is one of the classical dynamical systems. The logistic map has been extensively studied and other properties can be found in [38] while some basic properties can be found in [39, 40].

Definition 3 The tent map is defined as

$$f_{T,}(x, \mu) = \begin{cases} \mu x, & \text{for } x < 1/2, \\ \mu(1 - x), & \text{for } x \geq 1/2, \end{cases} \tag{2}$$

where parameter $\mu \in [0, 2] \subset \Re$.

The logistic and tent maps are obviously unimodal ones, as they are continuous on $\mathcal{I}$ with a single critical point $c_0 = 0.5$ and they increase for $x \in [0, 0.5)$ and they decrease for $x \in [0.5, 1]$. Their bifurcation diagrams using α and μ as control parameters demonstrate a very rich dynamics [41, 42].

Example 1 The following quadratic map:

$$f_Q(x, \gamma) = \gamma(1 - 2x) \begin{cases} x, & \text{if } x < 0.5, \\ (x - 1), & \text{other case,} \end{cases} \tag{3}$$

is the bimodal map in the sense of the Definition 1. As a matter of fact, the map given by Eq. (3) has three critical points and two of them are $c_0 = 0.25$ and $c_1 = 0.75$ located at intervals $\mathcal{I}_0 = [0, 0.5)$ and $\mathcal{I}_1 = [0.5, 1]$, respectively. The other critical point $c = 0.5$ due to $f'_Q(0.5)$ does not exist. Notice that this critical point does not satisfied the Definition 1. Thus the map given by Eq. (3) is a bimodal map.
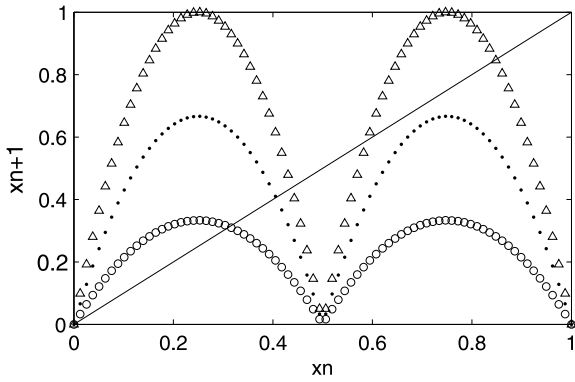
Fig. 1 Difference map for different valued of β: 1.333 (*line formed by circles*), 2.666 (*dotted line*) and 4 (*line formed by triangles*)

Definition 4 (Devaney's Definition of Chaos) [14] Let $(X; d)$ be a metric space. Then, a map $f : X \to X$ is said to be *Devaney-chaotic* on X if it satisfies the following conditions.

1. f has *sensitive dependence on initial conditions*. That is, there exists a certain $\epsilon > 0$ such that, for any $x \in X$ and $\delta > 0$, there exists some $y \in X$ where the distance $d(x; y) < \delta$ and $m \in \aleph = \{1, 2, 3, \ldots\}$ so that the distance $d(f^m(x); f^m(y)) > \epsilon$.
2. f is *topologically transitive*. That is, for any pair of open sets $U, V \subset X$, there exists a certain $m \in \aleph$ such that $f^m(U) \bigcap V \neq \emptyset$.
3. f has *dense distribution of the periodic orbits*. That is, suppose Y is the set that contains all periodic orbits of f, then for any point $x \in X$, there is a point y in the subset Y arbitrarily close to x.

The concept of neighborhood of a point $x \in X$ is important for demonstrating the second condition of Devaney's definition of chaos and is given as follows.

Definition 5 A *neighborhood* of a point $x \in X$ is a set $N_\delta(x)$ consisting of all points $y \in X$ such that the distance $d(x, y) < \delta$. The number δ is called the *radius* of $N_\delta(x)$.

3 Difference map

The main contribution of this paper is to present the so-called difference map and to provide its implementation as an electronic circuit. The difference map, denoted as $f_D(x, \beta)$, will be a particular case of the
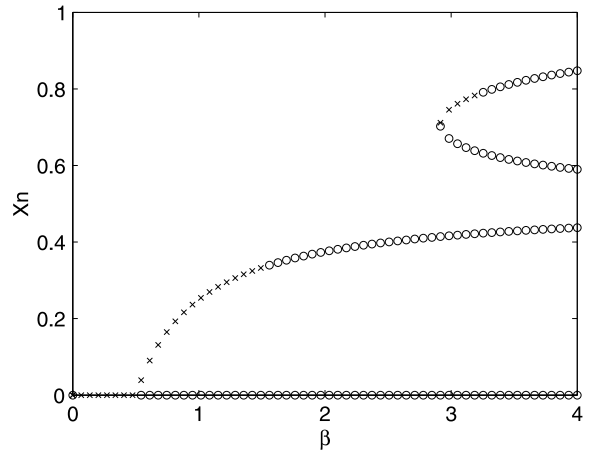

Fig. 2 Stability of the fixed points. The *asterisks* and *circles* denote stable and unstable fixed points, respectively

above described bimodal quadratic map equation (3) denoted $f_Q(x, \gamma) : [0, 1] \to [0, 1]$ with $\gamma = 2\beta$, where parameter $\beta \in [0, 4] \subset \Re$. This difference map is constructed based on the difference between logistic map and tent map, which explains such a terminology. More precisely, consider the following.

Definition 6 Consider the logistic and tent maps with maximum bifurcation parameters $\alpha = 4$, $\mu = 2$, respectively. Defined $f_D(x, \beta)$ as the difference between these two maps multiplied by the parameter $\beta \in [0, 4]$, namely, $f_D(x, \beta) = \beta(f_L(x, 4) - f_T(x, 2))$, i.e.:

$$f_D(x, \beta) = \begin{cases} 2\beta x(1 - 2x), & \text{for } x < \frac{1}{2}; \\ 2\beta(x - 1)(1 - 2x), & \text{for } x \geq \frac{1}{2}. \end{cases} \quad (4)$$

Indeed, the difference map defined in the Definition 6 is exactly the bimodal map equation (3) with $\gamma = 2\beta$. Now, β is a new bifurcation parameter which amplifies the difference between the logistic map and the tent map. This new parameter belongs to the interval [0, 4], notice that for $\beta = 4$ the difference map $f_D(x, \beta) : [0, 1] \to [0, 1]$. Figure 1 shows the difference map given by Eq. (4) for different values of β: 1.333 (line formed by circles), 2.666 (dotted line) and 4 (line formed by triangles). Notice that the difference map always has a fixed point at 0 and it can have others depending on the value of β at $\frac{2\beta-1}{4\beta}$, $\frac{6\beta-1-\sqrt{4\beta^2-12\beta+1}}{8\beta}$ and $\frac{6\beta-1+\sqrt{4\beta^2-12\beta+1}}{8\beta}$.

To analyze the behavior of the discrete-time dynamical system we put the map as its right hand side,
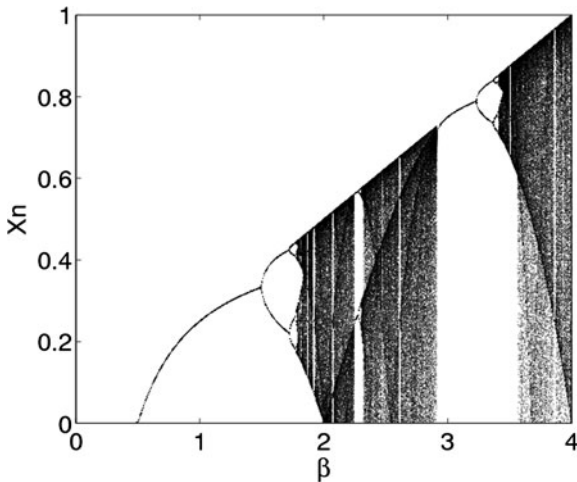
Fig. 3 Bifurcation diagram for the difference map given by Eq. (4)

Fig. 4 Lyapunov exponent of the difference map

i.e. the system

$$x_{k+1} = f_D(x_k, \beta), \quad \text{for } x_0 \text{ given and } k = 0, 1, 2, 3, \dots$$

The difference map can behave as a bimodal or unimodal map according to the β bifurcation parameter value. For example, if $\beta = 2$, then for any initial condition $x_0 \in [0, 1]$, $f_D(x, \beta)$ behaves after the first iteration as an unimodal map $f_D(x, \beta) : [0, 0.5] \to [0, 0.5]$. The stability of fixed points of the difference map can be attractive or repulsive as is shown in Fig. 2. An asterisk denotes an attractive fixed point and a circle denotes a repulsive fixed point. The fixed point located at zero is attractive for $\beta \in [0, 0.5]$ and repulsive for $\beta \in [0.5, 4]$. The second fixed point is given by $\frac{2\beta-1}{4\beta}$ which is attractive for $\beta \in [0.5, 1.495)$ and repulsive for $\beta \in [1.495, 4]$. The third fixed point located at $\frac{6\beta-1-\sqrt{4\beta^2-12\beta+1}}{8\beta}$ is always repulsive for $\beta \in [2.915, 4]$ and last one given by $\frac{6\beta-1+\sqrt{4\beta^2-12\beta+1}}{8\beta}$ is attractive for $\beta \in [2.915, 3.235)$ and repulsive for $\beta \in [3.235, 4]$.

It is well known that an attractive fixed point does not let oscillations meanwhile a repulsive fixed point can yield periodic orbits and even chaotic orbits. Figure 3 shows a bifurcation diagram of the orbit of the difference map $f_D(x_0, \beta)$, which is on $[0, 1] \times [0, 4]$. Two sequences of the period-doubling bifurcations appear approximately at $\beta = 1.5$ and $\beta = 3.2312$. For $\beta \in [0, 2]$ the difference map resembles to the logistic map but it oscillates in the interval $[0, 0.5]$, and for
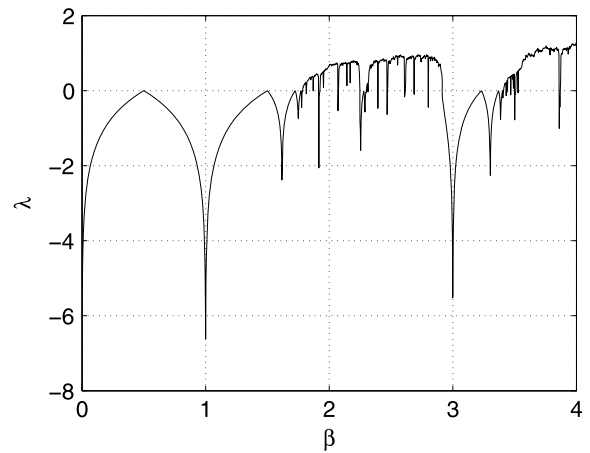
$\beta \in [2, 4]$ it behaves as a bimodal map and it can oscillate in the interval $[0, 1]$.

The Lyapunov exponent, which is denoted by λ, gives the global stability of the system equation (3) and it is shown in Fig. 4. For $\beta \in [0, 0.5]$ the system only has a fixed point which is attractive and $\lambda < 0$, the orbit converges to the fixed point. For $\beta \in [0.5, 1.5)$ the system has two fixed points: one attractive and the other repulsive and $\lambda < 0$ due to the orbit converges to the attractive fixed point but when $\beta = 1.5$ the system has a bifurcation and the value of $\lambda = 0$. For $\beta \in (1.5, 2.915)$ the system has two fixed points and both are repulsive and $\lambda < 0$ when the orbit periodically oscillates or $\lambda > 0$ when the orbit oscillates chaotically. For $\beta \in (2.915, 3.235)$ the system has four fixed points and three of them are repulsive and the other fixed point is attractive, $\lambda < 0$, thus the orbit converges to the attractive fixed point again and also when $\beta = 3.235$ another bifurcation occurs and therefore $\lambda = 0$. For $\beta \in (3.235, 4]$ the system maintains its four fixed points but now all of them are repulsive. The orbit oscillates periodically or chaotically when $\lambda < 0$ and $\lambda > 0$, respectively. It is worth mentioning that the Lyapunov exponent was defined for unimodal systems; however, it measures the average exponential rates of divergence or convergence of orbits no matter if the system is k-modal because the system is one dimensional.

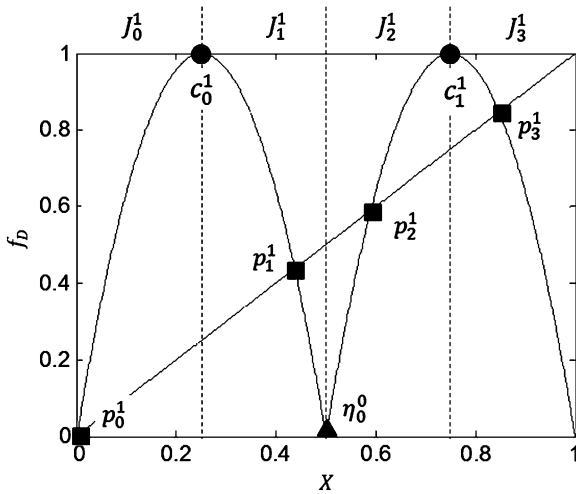**Theorem 1** *The difference map $f_D(x, \beta)$ is Devaney-chaotic on $[0, 1]$ for $\beta = 4$.*

Fig. 5 The difference map and the subintervals J_i^1, $i = 0$, 1, 2, 3. *Circles* denote critical points, *squares* denote fixed points and *triangles* denote η

Fig. 6 Distribution of the periodic orbits of period two, *circles* denote critical points, *squares* denote fixed points, and *triangles* denote η

Proof From Definition 4, we need to prove three conditions: (1) the sensitive dependence upon the initial condition, (2) the topological transitivity and (3) the dense distribution of the periodic orbits.

We start by demonstrating the last property. We need to prove that there exists a Y subset of the interval $I = [0, 1]$ constitutes for periodic orbits, and that Y is dense in I. The I interval can be divided by $J_0^1 = [0, c_0^1]$, $J_1^1 = [c_0^1, \eta_0^0 = 0.5]$, $J_2^1 = [\eta_0^0 = 0.5, c_1^1]$ and $J_3^1 = [c_1^1, 1]$ (see Fig. 5), and each intervals contains one fixed point of the difference map f_D, $\Delta^1 = \{p_0^1 = 0, p_1^1 = 0.4375, p_2^1 = 0.5899, p_3^1 = 0.8476\}$, respectively. These fixed points in the closed interval I belong to Y as periodic orbits of period one, where $c_0^1 = 0.25$ and $c_1^1 = 0.75$ are the critical points. Notice that $f_D : J_i^1 \to [0, 1]$, $i = 0, \ldots, 3$, then each subinterval resembles the difference map for f_D^2. Notice that $f_D(0) = f_D(0.5) = f_D(1) = 0$ and $f_D(c_0^1 = 0.25) = f_D(c_1^1 = 0.75) = 1$. The foregoing observation let us to infer that for all $x \in I$ and if $f_D^k(x) = 0.5$ then $f_D^{k+1}(x) = 0$.

The fixed points correspond to the intersection between f_D and the identity function $f_I(x) = x$. If we consider the intersection between the second iteration f_D^2 and f_I we find that these functions intersect at 16 points, the set of fixed points Δ^1 and a set of periodic points of period two Δ^2. Now the interval I consisted of 16 subintervals $J_0^2 = [0, c_0^2]$, $J_1^2 = [c_0^2, \eta_0^1]$, $J_2^2 = [\eta_0^1, c_1^2]$, $J_3^2 = [c_1^2, c_0^1]$, $J_4^2 = [c_0^1, c_2^2]$, $J_5^2 = [c_2^2, \eta_1^1]$, $J_6^2 = [\eta_1^1, c_3^2]$, $J_7^2 = [c_3^2, 0.5]$,
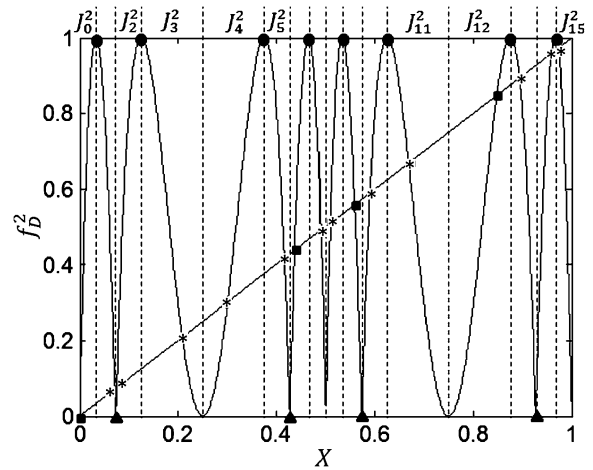
$J_8^2 = [0.5, c_4^2]$, $J_9^2 = [c_4^2, \eta_2^1]$, $J_{10}^2 = [\eta_2^1, c_5^2]$, $J_{11}^2 = [c_5^2, c_1^1]$, $J_{12}^2 = [c_1^1, c_6^2]$, $J_{13}^2 = [c_6^2, \eta_3^1]$, $J_{14}^2 = [\eta_3^1, c_7^2]$ and $J_{15}^2 = [c_7^2, 1]$. Figure 6 shows the subintervals $J_i^2, i = 0, 1, 2, \ldots, 15$, the fixed points are marked with squares and the periodic points with period two with asterisk, $\Delta^2 = p_0^2, p_1^2, p_2^2, p_3^2, \ldots, p_{11}^2$. The set $\{c_0^2, c_1^2, c_2^2, c_3^2, c_4^2, c_5^2, c_6^2, c_7^2\}$ contains the critical points of f_D^2 and $\eta_i^1 = f_D(x) = 0.5$, $i = 0, \ldots, 3$. The periodic points of period one and two belong to $Y \supset \Delta^1 \cup \Delta^2$. In general, the intersections between f_D^n and f_I give the periodic points of period n and may be periodic points of less period. I is comprised by subintervals J_i^n, $i = 0, \ldots, 4^n - 1$ and the end points of the intervals are given by the critical points of f_D^k, $\eta^{k-1} = f_D^{k-1}(x) = 0.5$, $k = 1, \ldots, n$, and the previous end points. The particularity is that each subinterval J_i^n contains at least a periodic point and $|J_i^n| \to 0$ when n $\to \infty$. Thus for any $x \in I$, there is a point y in the subset Y arbitrarily close to x, so this proves that periodic points are dense in $[0, 1]$.

In order to demonstrate that f_D is *topologically transitive*. We consider a pair of open sets $N_\delta(y_1)$, $N_\delta(y_2) \subset I$, for any $y_1, y_2 \in I$, we need to show that there exists a certain $m \in N = \{1, 2, 3, \ldots\}$ such that $f_D^m(N_\delta(y_1)) \cap N_\delta(y_2) \neq \emptyset$, i.e., we need to show that at least one orbit with initial condition $x_0 \in N_\delta(y_1)$ evolves to $N_\delta(y_2) \ni f_D^m(x_0)$. First we consider two open sets $N_\delta(y_1)$ and $N_\delta(y_2)$ arbitrarily located at I as is shown in Fig. 7. In the previous paragraphs we discuss that each subintervals J_i^k tends to zero when k
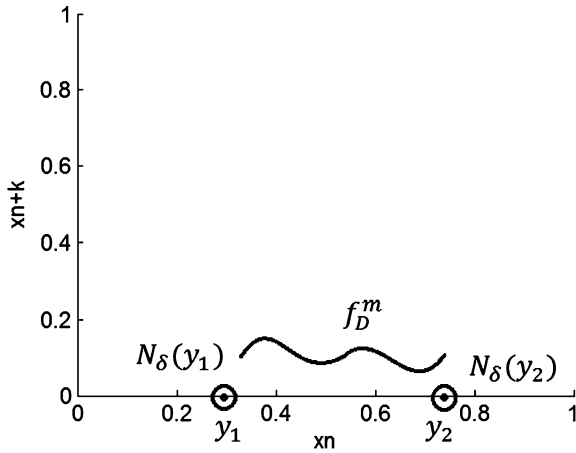
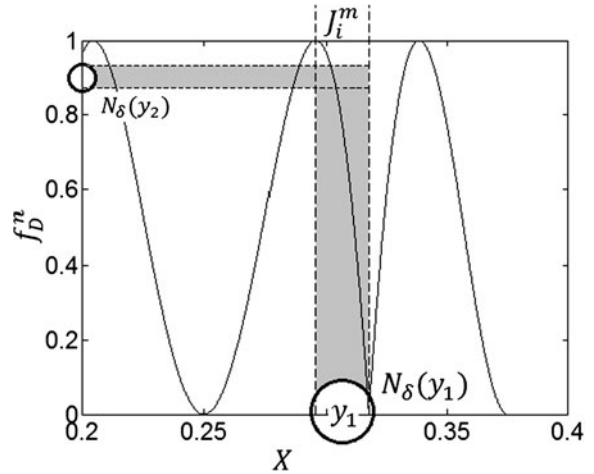**Fig. 7** There exists an orbit such that two points with a neighborhood comes arbitrarily close

Fig. 9 A zoom of Fig. 8 in order to appreciate the transitivity of an orbit of period n where $f(J_i^m) \supseteq I \supset N_\delta(y_1)$
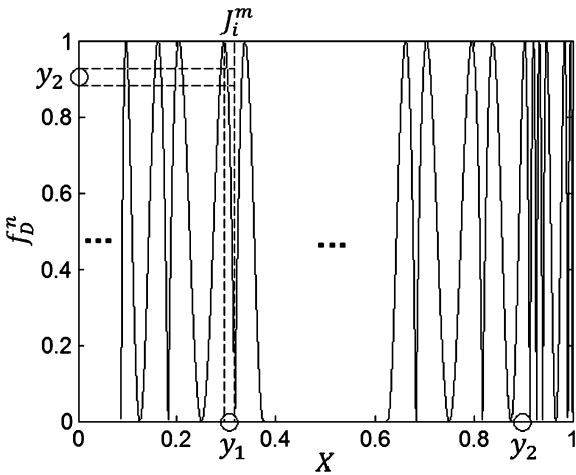

Fig. 8 Transitivity of an orbit of period n (f_D^n) of difference map

Fig. 10 Circuit diagram of an electronic map

tends to infinity, also we know that each subinterval J_i^k is mapped onto the interval I, $f_D^k : J_i^k \to I$. Thus, consider a subinterval $J_i^m \subset N_\delta(y_1)$. as is shown in Figs. 8 and 9. Accordingly $f(J_i^m) = I \supset N_\delta(y_2)$ then $f_D^m(x_0) \in N_\delta(y_2)$, for any $x_0 \in N_\delta(y_1)$, this proves that f_D is topologically transitive.

Finally, we need to demonstrate *sensitive dependence on initial conditions* of the difference map, so that we start to define $\epsilon = |I|/2$, where $|I| = 1$, such that for any $x_{01} \in I$ and any $\delta > 0$ there is a $x_{02} \in N_\delta(x_{01})$ such that the distance between $|f_D^m(x_{01}) - f_D^m(x_{02})| \geq \epsilon$.

So if we consider the subinterval J_i^{m-1} such that $J_i^{m-1} \subset N_\delta(x_{01})$ then there is a $x_{02} \in J_i^{m-1}$ such that
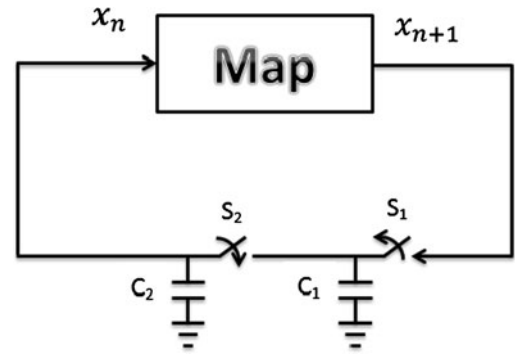
$|f_D^m(x_{01}) - f_D^m(x_{02})| \geq 1/2$. Thus we have sensitive dependence on initial conditions is important to note that the definition of sensitivity does not require that the orbit of x_{02} remains far from x_{01} for all iterations. We only need one point on the orbit to be far from the corresponding iterate of x_{01}.

Now the proof is completed. □

Remark 3 The Li–Yorke theorem can be used to demonstrate chaos, but for the purposes of this paper Theorem 1 is sufficient.

4 Electronic implementation of the difference map

An electronic circuit of a discrete map is made up by the implementation of two parts: (1) the discrete map circuit, and (2) the iterative process circuit, see

Fig. 11 Block diagram of
the difference map used to
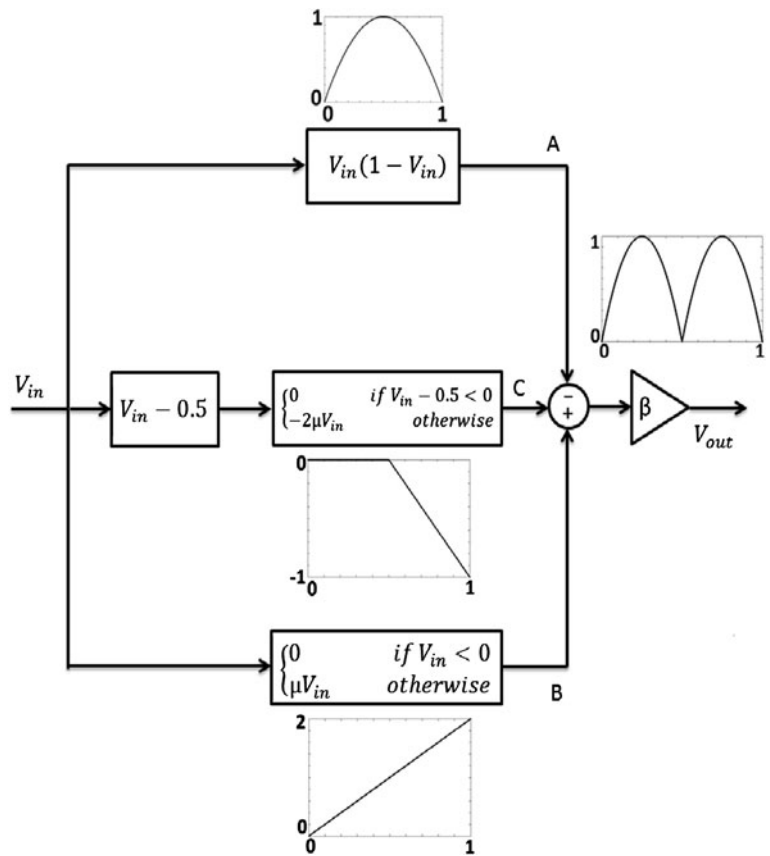construct the electronic
circuit

Fig. 10. Some electronic implementations are based on microprocessor or microcontrollers in one or both of its parts; however this leads to a discrete space. From Definition 4, one can immediately see that no map is Devaney-chaotic if X is a discrete space. Thus, a chaotic system needs to be implemented electronically by analog devices. First we will focus on explaining the circuit of the difference map.

The experimental development of this map is achieved by means of electronic devices as multipliers, operational amplifiers, diodes, and resistors. In the same spirit that other implementations of this kind of circuits [19, 43] analog multipliers have been employed with a normalization of the signal by a factor of about 10. This normalization is necessary because of the physical restrictions in the analog multiplier. The starting point is a block diagram of the difference map that is shown in Fig. 11. The output of the electronic circuit has three branches: The first generates the logistic map (node A) and the last two correspond to the tent map (node B and C). Typically, these circuits contain several operational amplifiers, which

perform linear operations (e.g., integration and summation), as well as a couple of integrated circuits that perform the nonlinear operations (i.e., multiplication). Here, we describe a new circuit contains active components, speeds of radio frequencies, and is capable of reproducing the transition from steady state to chaos as observed in the difference map equation when the bifurcation parameter is varied.

Figure 12 shows a schematic diagram of the electronic circuit realization of the difference map. The output of the circuit is analyzed using the voltages at the nodes: A, B, C, D.

The A node voltage is given by the $M1$ multiplier which has four input terminals (x_1, x_2, y_1, y_2) and an output terminal given by $W = \frac{(x_1 - x_2)(y_1 - y_2)}{10}$. Inputs $x_1 = V_{in}(R_2 R_4)/(R_1 R_3)$ and $y_2 = V_{in}(R_2 R_6)/(R_1 R_5)$ are given by operational amplifiers U2 and U3, respectively. Inputs x_2 and y_1 are 0 V and 5 V, respectively. Hence, the output at A node is given by

$$V_A = \left(V_{in} \frac{R_2 R_4}{R_1 R_3} \right) \left(5 - V_{in} \frac{R_2 R_6}{R_1 R_5} \right) / 10, \tag{5}$$

Fig. 12 Schematic diagram
of the difference map
electronic circuit
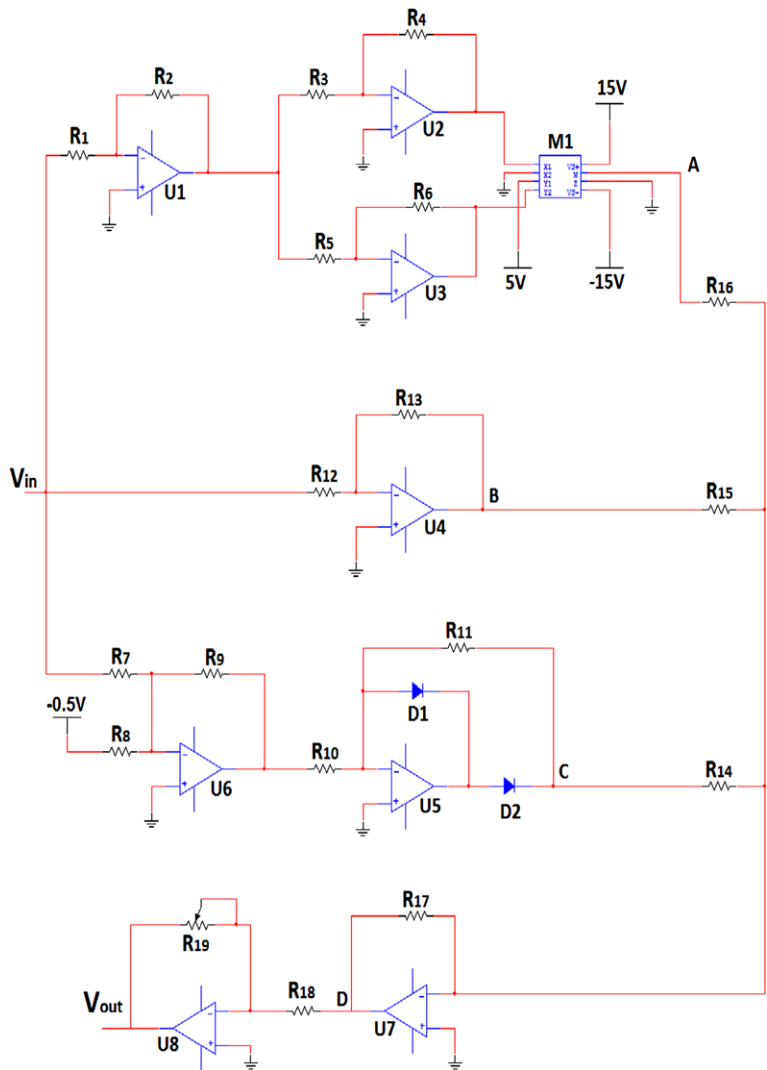
the A node voltage is $V_{in}(1 - V_{in})$ after evaluating components values of the Table 1, this signal corresponds to the logistic map f_L without considering the α bifurcation parameter.

The B node voltage is given by the U4 amplifier output which is fed back to the inverting input, the output voltage is

$$V_B = -V_{in} R_{13}/R_{12}. \tag{6}$$

The C node voltage is given by the U5 amplifier output which is a piecewise linear signal, then

$$V_C = \begin{cases} 0, & \text{for } V_{in} < \frac{R_7}{2R_8}; \\ \frac{R_{11}}{R_{10}}\left(\frac{R_9 V_{in}}{R_7} - \frac{R_9}{2R_8}\right), & \text{for } V_{in} \geq \frac{R_7}{2R_8}. \end{cases} \tag{7}$$

Equations (6) and (7) correspond to the tent map, remember that $f_T(x, \mu)$ is defined by two parts, to ensure that the map is symmetric the bifurcation parameter μ must be the same on both sides. We can see that μ is given by R_{13}/R_{12} and $R_{11}/(2R_{10})$. This yields the following restrictions: $R_{11} = 2R_{13}$ and $R_{10} = R_{12}$.

The U7 amplifier output is the adding of A, B and C node voltages which correspond to D node voltage, giving

$$V_D = -R_{17}\left(\frac{V_A}{R_{16}} + \frac{V_B}{R_{15}} + \frac{V_C}{R_{14}}\right), \tag{8}$$

it is worth mentioning that the ratio R_{17}/R_{16} is the parameter $\alpha = 4$. Thus, the D node voltage is $(-f_L + f_T)$ that is indeed the difference map invested

Table 1 The values of the electronic components employed in the construction of the difference map electronic circuit

Device	Value
$R_1, R_3, R_5, R_6, R_7, R_8, R_9,$	
$R_{10}, R_{12}, R_{16}, R_{18}$	10 kΩ Resistor
R_4	4 kΩ Resistor
$R_{11}, R_{14}, R_{15}, R_{17}$	40 kΩ Resistor
R_{13}	20 kΩ Resistor
R_{19}	40 kΩ Potentiometer
D1, D2	1N4148 Diode
U1, U2, U3, U4, U5, U6, U7, U8	TL084 Op. Amp.
M1	AD633 Multiplier

without taking into account the bifurcation parameter β.

Finally, the V_{out} voltage is given by the U8 inverting amplifier, the output is $(R_{19}/R_{18})V_D$. Assuming ideal performance from all components, the circuit output in Fig. 12 is modeled by the following equation:

$$V_{\text{out}} = \frac{R_{19}}{R_{18}} \begin{cases} 4V_{\text{in}}(1 - V_{\text{in}}) - 2V_{\text{in}}, & \text{for } V_{\text{in}} < \frac{1}{2}\,\text{V}; \\ 4V_{\text{in}}(1 - V_{\text{in}}) + 2V_{\text{in}} - 2, & \\ \quad \text{for } V_{\text{in}} \geq \frac{1}{2}\,\text{V}. \end{cases} \quad (9)$$

Then, Eq. (4) can be derived from Eq. (9) by the change of variables $V_{\text{in}} = x_n$, $V_{\text{out}} = x_{n+1}$ and $\beta = R_{19}/R_{18}$.

The second part of the circuit is responsible for make the iterative operation, (see Fig. 10), this circuit considers a microcontroller PIC16F88 of Microchip, and two hold and sample LF398 of National Semiconductors in order to hold the V_{out} signal given by Eq. (9). That is, hold and sample circuits have been used as an analog memory in order to store the value of x_k and get x_{k+1}. In this way the electronic circuit shown in Fig. 12 generates the iterative operation. Obviously, there are different ways to perform this iterative operation, but this is a matter that depends on the design of the application. Figure 13 shows a schematic diagram for this part of the circuit, one can see that each device LF398 (U1 and U2) has an input for activation, the signal for both hold and sample devices come from the microcontroller PIC16F88.

The time of each trigger to activate devices is defined for the designer, in this case we set 20 ms between each shot, where the duration of each shot is 1 ms, these times are programmed into the microcontroller and can vary depending on the application.
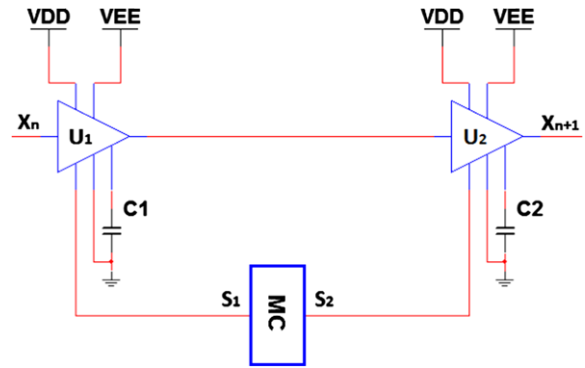

Fig. 13 Schematic diagram of the iterative circuit, U1 and U2 are LF398 and the MC microcontroller is a PIC16F88
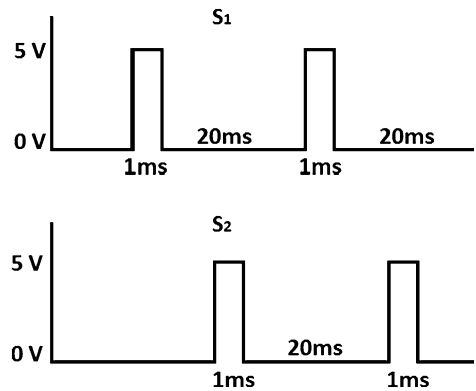

Fig. 14 Times of activation for hold and sample

Figure 14 shows a diagram with the time of activation of each hold and sample device.

Once both circuits are tuned in correct operation the difference map begins its iterative process. Figure 15 shows a time series for $\beta = 4$. In spite of parasitic reactance, finite bandwidth of active components, and other experimental perturbations, the presented electronic circuit closely displays the behavior of the mathematical model given by Eq. (4). We have implemented this design on a printed circuit board (PCB) manufactured in our laboratory. In the experimental circuit the TL084 operational amplifiers and LF398 hold and sample devices have been supplied with a power source at ± 15 V and soldered directly to the PCB without a socket, also a source power of -0.5 V is used for proper operation of the tent map. The voltage V_{dc} has been supplied by a variable dc supply with an output range of 0–15 V.

The value of the bifurcation parameter β can be fixed at certain value by simply adjusting the poten-
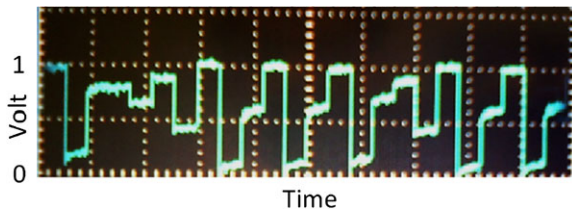
Fig. 15 The time series with chaotic dynamics generated by the tent map for $\beta = 4$
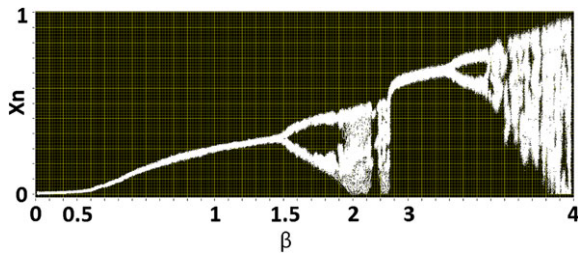

Fig. 16 Experimental bifurcation diagram for the difference map

tiometer R_{19} located in the operational amplifiers U8. In order to explore the full range of the dynamics accessible to this circuit, we have experimented with different values for R_{19}. The value of this potentiometer has been adjusted in the closed interval $[0\ \Omega, 40\ k\Omega]$. Then the value of β has been varied to obtain the bifurcation diagram shown in Fig. 16, where fixed points, periodic oscillations, cascade of period-doubling bifurcations and chaos can be clearly seen. It is possible to see that the circuit exhibits the entire range of behaviors of the difference map. In fact, our experimental results of the dynamics of this circuit are found to be in good agreement with numerical simulations.

Note that this circuit only produce a bimodal map in order to construct a circuit with k modal we need to use another technique as comparator circuits in order to define the partition of the space and after this construct a logistic map on each partition using multipliers devices.

5 Conclusion

In this paper we introduced a new discrete-time dynamical system of one dimension based on the difference of the logistic and tent map. This map is a bimodal map that presents chaotic behavior according to its Lyapunov exponent. One of the main properties of this map is that it can show the behavior of a unimodal map or a bimodal map by setting the β parameter. A difference map electronic circuit has been presented here and its implementation using only analog components as operational amplifiers, multipliers, diodes, and resistors was also provided. Thus, this design can be manufactured in just one chip because the final electronic circuit contains only semiconductors and passive components. Its experimental behavior was tested and compared with the numerical behavior given by the difference map equation 4. The circuit replicates the whole known range of behaviors of the difference map and it has many potential applications, for example: random number generation, frequency hopping, ranging, and spread-spectrum communications. As the outlook for further research, the possibility of encryption using stream ciphers based on the analog circuit is considered. This is the object of currently ongoing research.

References

1. Mengue, A.D., Essimbi, B.Z.C.: Secure communication using chaotic synchronization in mutually coupled semiconductor lasers. Nonlinear Dyn. **70**(2), 1241–1253 (2012)
2. Wang, X.-y., Qin, X., Jessa, M.: A new pseudo-random number generator based on CML and chaotic iteration. Nonlinear Dyn. **70**, 1589–1592 (2012)
3. Patidar, V., Sud, K.K., Pareel, N.K.: A pseudo random bit generator based on chaotic logistic map and its statistical testing. Informatica **33**, 441–452 (2009)
4. Yuan, X., Xie, Y.-X.: A design of pseudo-random bit generator based on single chaotic system. Int. J. Mod. Phys. C **23**(3), 1250024 (2012)
5. Zou, A.-M., Kumar, K.D., Pashaie, R., Farhat, N.H.: Neural network-based adaptive output feedback formation control for multi-agent systems. Nonlinear Dyn. **70**, 1283–1296 (2012)
6. Chen, Y., Fei, S., Zhang, K.: Stabilization of impulsive switched linear systems with saturated control input. Nonlinear Dyn. **69**, 793–804 (2012)
7. Mazloom, S., Eftekhari-Moghadam, A.M.: Color image encryption based on coupled nonlinear chaotic map. Chaos Solitons Fractals **42**, 1745–1754 (2009)

8. Shatheesh Sam, I., Devaraj, P., Bhuvaneswaran, R.S.: An intertwining chaotic maps based image encryption scheme. Nonlinear Dyn. **69**, 1995–2007 (2012)

9. Farschi, S.M.R., Farschi, H.: A novel chaotic approach for information hiding in image. Nonlinear Dyn. **69**, 1525–1539 (2012)

10. Hussain, I., Shah, T., Gondal, M.A.: Image encryption algorithm based on PGL(2, GF(2^8)) S-boxes and TD-ERCS chaotic sequence. Nonlinear Dyn. **70**, 181–187 (2012)

11. Kwok, H.S., Tang, W.K.S.: A fast image encryption system based on chaotic maps with finite precision representation. Chaos Solitons Fractals **32**, 1518–1529 (2007)

12. Campos-Cantón, E., Femat, R., Pisarchik, A.N.: A family of multimodal dynamic maps. Commun. Nonlinear Sci. Numer. Simul. **9**, 3457–3462 (2011)

13. Devaney, R.: An Introduction to Chaotic Dynamical Systems, 2nd edn. Westview Press, Boulder (2003)

14. Kahng, B.: Redefining chaos: Devaney-chaos for piecewise continuous dynamical systems. Int. J. Math. Models Methods Appl. Sci. **3**(4), 317–326 (2009)

15. Li, T.-Y., Yorke, J.A.: Period three implies chaos. Am. Math. Mon. **82**(10), 985–992 (1975)

16. Li, C., Chen, G.: Estimating the Lyapunov exponents of discrete systems. Chaos **14**, 343–346 (2004)

17. Sano, M., Sawada, Y.: Measurement of the Lyapunov spectrum from a chaotic time series. Phys. Rev. Lett. **55**, 1082–1085 (1985)

18. Yang, C., Wu, C.Q., Zhang, P.: Estimation of Lyapunov exponents from a time series for n-dimensional state space using nonlinear mapping. Nonlinear Dyn. **69**, 1493–1507 (2012)

19. Suneel, M.: Electronic circuit realization of the logistic map. Sadhana **31**, 69–78 (2006)

20. Campos-Cantón, I., Campos-Cantón, E., Murguía, J.S., Rosu, H.C.: A simple electronic circuit realization of the tent map. Chaos Solitons Fractals **1**, 12–16 (2009)

21. Senani, R., Gupta, S.: Implementation of Chua's chaotic circuit using current feedback op-amps. Electron. Lett. **34**(9), 829–830 (1998)

22. Banerjee, T.: Single amplifier biquad based inductor-free Chua's circuit. Nonlinear Dyn. **68**, 565–573 (2012)

23. Gandhi, G.: An improved Chua's circuit and its use in hyperchaotic circuit. Analog Integr. Circuits Signal Process. **46**(2), 173–178 (2006)

24. Matsumoto, T.: A chaotic attractor from Chua's circuit. IEEE Trans. Circuits Syst. I **31**(12), 1055–1058 (1984)

25. Chua, L., Komuro, M., Matsumoto, T.: The double scroll family: parts I and II. IEEE Trans. Circuits Syst. I **33**, 1073–1118 (1986)

26. Radwan, A., Soliman, A., El-Sedeek, A.: MOS realization of the double-scroll-like chaotic equation. IEEE Trans. Circuits Syst. I **50**(2), 285–288 (2003)

27. Yalcin, M., Suykens, J., Vandewalle, J., Ozoguz, S.: Families of scroll grid attractors. Int. J. Bifurc. Chaos **12**(1), 23–41 (2002)

28. Kilic, R.: On current feedback operational amplifier-based realization of Chua's circuit. Circuits Syst. Signal Process. **22**(5), 475–491 (2003)

29. Kilic, R.: Experimental study of CFOA-based inductorless Chua's circuit. Int. J. Bifurc. Chaos **14**, 1369–1374 (2004)

30. O'Donoghue, K., Forbes, P., Kennedy, M.: A fast and simple implementation of Chua's oscillator with cubic-like nonlinearity. Int. J. Bifurc. Chaos **15**, 2959–2972 (2005)

31. Lü, J., Chen, G.: Generating multiscroll chaotic attractors: theories, methods and applications. Int. J. Bifurc. Chaos **16**(4), 775–858 (2006)

32. Addabbo, T., Alioto, M., Fort, A., Rocchi, S., Vignoli, V.: The digital tent map: performance analysis and optimized design as a low-complexity source of pseudorandom bits. IEEE Trans. Instrum. Meas. **55**(5), 1451–1458 (2006)

33. Perez, G., Cerdeira, H.: Extracting messages masked by chaos. Phys. Rev. Lett. **74**, 1970–1973 (1995)

34. Short, K.M., Parker, A.T.: Unmasking a hyperchaotic communication scheme. Phys. Rev. E **58**, 1159–1162 (1998)

35. Zhou, C., Lai, C.H.: Extracting messages masked by chaotic signals of time-delay systems. Phys. Rev. E **60**, 320–323 (1999)

36. Zhang, Y., Li, C., Li, Q., Zhang, D., Shu, S.: Breaking a chaotic image encryption algorithm based on perceptron model. Nonlinear Dyn. **69**, 1091–1096 (2012)

37. Verhulst, P.F.: Notice sur la loi que la population poursuit dans son accroissement. Corresp. Math. Phys. **10**, 113–121 (1838)

38. Holmgren, R.A.: A First Course in Discrete Dynamical Systems. Springer, New York (1996)

39. Lynch, S.: Dynamical Systems with Applications. Birkhäuser, Boston (2010)

40. Wu, C.W., Rul'kov, N.F.: Studying chaos via 1-D maps—a tutorial. IEEE Trans. Circuits Syst. I **40**, 707–721 (1993)

41. Li, C.: A new method of determining chaos-parameter-region for the tent map. Chaos Solitons Fractals **21**, 863–867 (2004)

42. Huang, W.: On complete chaotic maps with tent-maps-like structures. Chaos Solitons Fractals **24**, 287–299 (2005)

43. Blakely, J.N., Eskridge, M.B., Corron, N.J.: A simple Lorenz circuit and its radio frequency implementation. Chaos **17**, 023112 (2007)